Environmental Science & Technology

Article

Cite This: Environ. Sci. Technol. 2019, 53, 13219−13227

pubs.acs.org/est

Erosion Behavior of Different Microplastic Particles in Comparison to Natural Sediments

Kryss Waldschläger* and Holger Schüttrumpf

Institute of Hydraulic Engineering and Water Resources Management, RWTH Aachen University, Mies-van-der-Rohe-Str. 17, 52074 Aachen, Germany

Supporting Information

ABSTRACT: Microplastic (MP) has been detected in marine, limnic, terrestrial, and atmospheric environments. However, rivers are often only seen as transport paths for MPs from inland sources to the oceans, although transport rates in rivers can hardly be determined yet. MP in rivers can either be transported, or it settles to the bottom of the river and either remains there or is remobilized again at higher flow velocities. This remobilization, also known as erosion, depends on the critical shear stress of a particle and is influenced by the particle properties and the sediment bed. In this study, the critical shear stresses of 14 MP particles with different shapes, densities, and particle sizes on different sediment beds were experimentally determined and subsequently compared with the basic principles of erosion from sediment transport. Critical shear stresses of the MP particles were between 0.002 and 0.233 N/m^2, depending on particle and sediment properties. Furthermore, the hiding-exposure effect was transferred to MPs and an equation was developed to determine the critical shear stress of different MP particles on natural sediment beds.

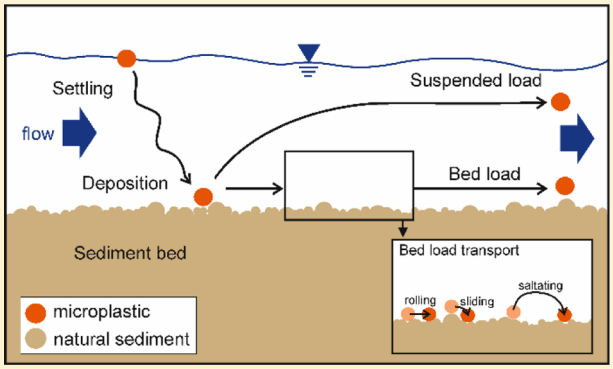

INTRODUCTION

Microplastic (MP) has already been reported in terrestrial,[1,2] marine,[3,4] and limnic environments[5,6] as well as in the atmosphere,[7,8] with the research focus recently shifting from marine to limnic compartments.[9,10] Although there are more and more studies on MP concentrations in rivers, the predominant transport mechanisms of MP have been investigated only sporadically.[6,11−13] For this reason, it has not yet been possible to make reliable statements about hotspots, transport routes, sources, and sinks of MPs in rivers.[2,14]

Recent studies assume that a large proportion of the MP input into the oceans occurs via rivers.[15] In rivers, however, MP is not only transported to the oceans, but it also settles onto the river bed, where it either accumulates or is remobilized again at higher flow rates such as during flood events (cf. Figure 1).[16] The extent to which this remobilization, known as erosion, depends on the MP particle properties and the natural sediment bed has not yet been researched.[17] However, a more detailed knowledge of erosion behavior is indispensable for a profound estimation of the transport capacities of MP in rivers, as the erosion behavior can be used to determine whether the MP particles are deposited and which flow velocity is necessary to remobilize the particles.

It is generally assumed that MPs in surface waters behave similarly to sediments.[18] However, whereas natural sediment has an average density of 2650 kg/m^3, the density of MP ranges between 20 and 1400 kg/m^3. Approximately half of all manufactured plastics are heavier than water and can therefore sink to the bottom without any further influence necessary.[19] In addition, MP particles have very diverse shapes such as pellets, fibers and fragments, whereas sediment consists mainly of almost round grains. Because of those strongly varying particle properties and insufficient knowledge of the prevailing transport mechanisms, a transferability of the basic principles from sediment transport is at least questionable.[20]

Therefore, Waldschläger and Schüttrumpf (2019)[12] compared the settling and rising behavior of different MP particles to that of natural sediments and were able to show that MPs' settling and rise velocities could only be calculated insufficiently with the equations from sediment transport. It should therefore be further examined whether MP differs from sediment in other transport mechanisms. Because of its significance for the transport rates of MP, and thus for global budgeting of MP in the aquatic environment, erosion behavior is of particular interest here. If MP behaves like natural sediment in water, conventional sediment transport models could be used in future. However, if the particles behave

Received: September 6, 2019
Revised: October 17, 2019
Accepted: October 18, 2019
Published: October 18, 2019

DOI: 10.1021/acs.est.9b05394
Environ. Sci. Technol. 2019, 53, 13219−13227

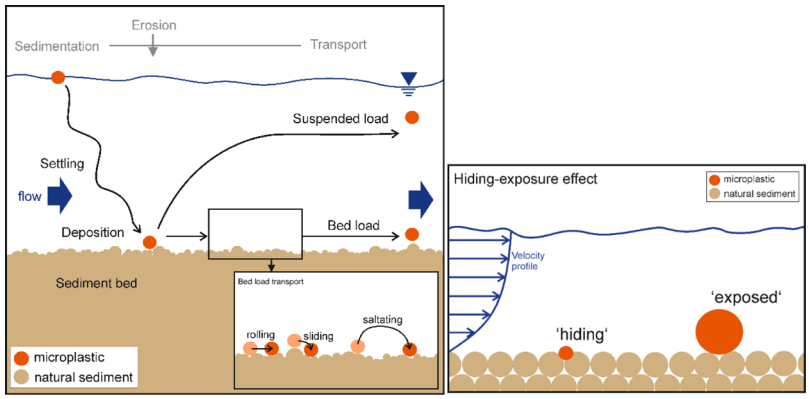

Figure 1. Behavior of MP particles in water (left); principle of the "hiding-exposure effect" (right).

differently, the original models must be adopted to ensure their informative value.

THEORETICAL BASICS

Sediment transport is generally divided into two different categories: suspended load and bed load transport. Suspended load is the process by which particles are transported through turbulence without contact with the river bed, that is, in suspension.[21] Bed load, on the other hand, is the transport of settled material by sliding, rolling, or saltating in a ballistic track directly above the ground (cf. Figure 1 on the left).[21] The first particle movement, that is the beginning of bed load transport, is generally defined as the start of erosion and occurs when the critical shear stress τ_c is reached.[22] Shear stress forms when a fluid moves along a solid boundary (here: sediment bed) and depends on the shear velocity of the fluid $u*$ and the density of the fluid ρ_w.[22]

The critical shear stress, that is the beginning of erosion, can be determined either experimentally or by using the Shields diagram, which is based on experimental tests with natural sediments conducted by Shields in 1936.[23] The Shields diagram separates the behavior of particles into "no motion" and "motion", wherein erosion is the transition from no motion to motion, illustrated by the Shields curve (cf. Figure 6). A particle moves if the force the flow exerts on the particle (i.e., lift and drag forces) gets higher than the grain resistance against the movement (i.e., the weight force). This relationship was described by Shields (1936) as a function of particle Reynolds number Re_p and Shields parameter θ. For the dimensionless Shields parameter θ, the following applies

$$\theta = \frac{\tau_0}{(\rho_s - \rho_f)gD} \tag{1}$$

τ_0: shear stress [N/m^2], ρ_p: particle density [kg/m^3], ρ_f: fluid density [kg/m^3], g: gravitational acceleration [m/s^2], D: particle diameter [m].

Particle Reynolds number Re_p [—], on the other hand, is defined by[23]

$$Re_p = \frac{u_* D}{\nu} \tag{2}$$

ν: kinematic viscosity of water [m^2/s], u_*: critical flow velocity,[24] calculated by $u_* = \sqrt{\frac{\tau_0}{\rho_p}}$.

The Shields diagram was originally developed exclusively for uniform sediments. In nature, however, mainly nonuniform sediments can be found, and the observation of MP particles on natural sediment is part of this research field. With nonuniform sediments, the so-called "hiding-exposure effect" occurs, which has several expressions: larger grains lying on a bed of smaller grains are more likely to be moved because of their exposed position (cf. Figure 1 on the right). Smaller grains on a bed of larger grains are shielded on the one hand by the bigger particles, but on the other hand also have a lower critical shear stress than the bed material and are thus more likely to be eroded than the sediment bed. The actual erosion behavior of nonuniform grains is therefore difficult to predict.[21]

The hiding-exposure effect is usually described by the following equation, which can be fitted via the variation of the hiding-exposure coefficient HE [—].[25]

$$\theta_{c,i}^* = \theta_c^* \left[\frac{D_i}{D_{50}}\right]^{-HE} \tag{3}$$

$\theta_{c,i}^*$: critical Shields parameter of the MP particle, θ_c^*: critical Shields parameter of the sediment bed, D_i [m]: representative MP particle diameter, D_{50} [m]: median grain size of the sediment bed.

On the basis of the principles described above, this study has therefore carried out physical experiments to determine the critical shear stress of different MP particles on uniform as well as nonuniform natural sediments. Afterward, the applicability of the Shields diagram is tested and the impact of the hiding-exposure effect on MP transport is analyzed.

MATERIALS AND METHODS

Test Setup. The critical shear stress of specific particles can be determined experimentally in a simulated benthic environment.[17,26,27] The annular flume of the Institute of Hydraulic Engineering and Water Resources Management (IWW) at RWTH Aachen University is particularly suitable for the investigation of erosion behavior. It can simulate an infinitely long stationary flow without using any pumps,[28] which allows to investigate the erosion behavior independently of turbulences that would have been caused by pumps.

The annular flume has an average diameter of 3.25 m, a width of 0.25 m, and can be filled up to a water height of 0.5 m. The supporting components of the apparatus are welded and bolted steel square tubes (blue) between which 8 mm thick float glass panes allow observation of the experiments and contactless measurements (cf. Figure 2).

DOI: 10.1021/acs.est.9b05394
Environ. Sci. Technol. 2019, 53, 13219−13227

The cover of the channel can be lowered to the water surface and is equipped with waterproof fluorescent tubes which ensure adequate lighting.

Figure 2. Annular flume of the Institute of Hydraulic Engineering and Water Resources Management at RWTH Aachen University.

Table 1. Selected Sediment Beds for the Experiments

sediment	grain size [mm]	D_{50} [mm]
no sediment		
medium sand	0.3−0.6	0.45
coarse sand	0.71−1.25	0.98
fine gravel	2−4	3
mixed sediment	mixing ratio 1:1:1 of the three sediments above	1.48

Various approaches are possible for the flow generation of an annular flume. Both the rotation of the flume itself, the drive through the cover, or both the movements of the inner and outer walls are possible. In case of the IWW annular flume, cover and flume are driven counter-rotating, which minimizes secondary flows in the water column.[28] The resulting movement can be compared to an endless Couette flow and a maximum shear stress of 0.9 N/m^2 can be achieved.

For the experiments, water, natural (uniform and nonuniform) sediment, and single MP particles were introduced into the annular flume. A water height of 325 mm was used in all experiments, as shear stresses were known from previous experiments[28] for this water height. Using a computer program specially developed for the annular flume at the IWW, the shear stress on the ground was then slowly increased by 0.0001 N/m^2 per s until the MP particle started to move.

Materials. A total of five different test setups were examined. At first, experiments without any sediment were carried out to represent a smooth bed, that is within canals. Afterward, three uniform sediments, each in one test setup, were installed in order to consider the erosion behavior in dependence of the grain sizes of sediment beds. For this purpose, representative sediments for river beds (medium sand, coarse sand, and fine gravel) were selected as seen in Table 1 and Figure 3. In the last test setup, the three uniform sediments were mixed in a ratio of 1:1:1, so that the erosion behavior of MP on a mixed river bed could be examined. All sediment beds were installed in a regular thickness of about 2 cm, to cover the bottom of the annular flume completely.

On the basis of investigations of MP compositions in rivers and production volumes of individual polymers, as described in Waldschläger and Schüttrumpf (2019),[12] MP particles were selected. They consist of the polymer types polyamide (PA), polystyrene (PS), polyethylene terephthalate (PET), and polyvinyl chloride (PVC), including shapes of pellets, spheres, fibers, and fragments. As the particles were initially placed on top of the sediment bed and to remain there, only polymer types heavier than water were selected. The particle sizes were between 0.5 and 8 mm and 14 different particles were analyzed (cf. Table 2). In the following, the equivalent diameter of the particles is always determined by the calculation of the nominal diameter by Wadell (1932),[29] which determines the equivalent sphere diameter of a particle on the basis of its three side lengths a, b, and c: $D_i = \sqrt[3]{acb}$. Consideration was given to using other equivalent particle diameters, but Wadell's diameter provided the most reasonable results.

Measurement Method. The aim of the experiments was to observe the onset of erosion and to assign the simultaneous bottom shear stress. The onset of erosion is hereby defined as the moment at which the MP particle started to move by either rolling, sliding, or saltating. Therefore, a GoPro HERO5 was installed on the inner frame of the annular flume, so that it rotated with the channel and therefore was always pointed at the same section of the sediment bed. Thus, the introduced MP particle was observed continuously. For the experiments, a camera setting of 1080p (90/90 fps) was used.

Some MP−sediment combinations could not be examined, as some MP particles had sand-like colors and, when the grain size of the sediment soil was similar to the size of the MP, a distinction was hardly possible. In total, between 11 and 14 different MP particles were investigated per sediment. In order to prove the reproducibility of the experiments, 10 runs were carried out per MP−sediment combination.

RESULTS AND DISCUSSION

In total, 620 individual runs were conducted. First, the reproducibility of the experiments was evaluated. For this purpose, the standard deviation s of the results from the 10 individual runs per particle and sediment bed was considered and compared to the mean shear stress $\bar{x}$ of the 10 runs. The standard deviation is determined using $s = \sqrt{\frac{\sum(x-\bar{x})^2}{n}}$.

The average standard deviation over all experiments is 37%. Although this value is relatively high, this was to be expected

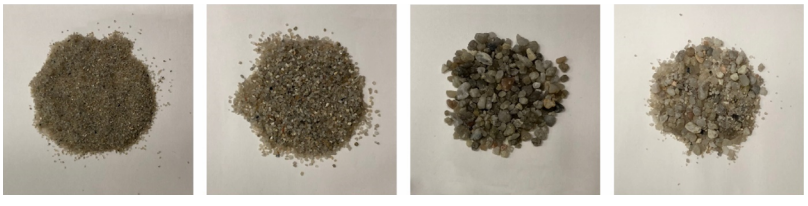

Figure 3. Selected sediment beds. From the left: medium sand, coarse sand, fine gravel, and mixed sediment.

DOI: 10.1021/acs.est.9b05394
Environ. Sci. Technol. 2019, 53, 13219−13227

Table 2. Investigated MP Particles and Their Particle Properties

polymer	abbreviation	density [kg/m^3]	shape	size [mm]	D_i [mm]
polystyrene	PS	1008	pellet cylindric	3 × 3 × 2	2.62
polystyrene	PS	1008	fragment	1−2	1.26
polystyrene	PS	1021	sphere	4.83	4.83
polyamide	PA	1107	fiber	diameter: 1 mm, length: 10 mm	2.15
polyamide	PA	1107	fiber	diameter: 0.5 mm, length: 10 mm	1.36
polyamide	PA	1140	pellet cubic	1 × 1 × 1	1.00
polyamide	PA	1140	pellet cubic	0.75 × 0.75 × 0.75	0.75
polyamide	PA	1140	pellet cylindric	1 × 1 × 1	1.00
polyvinyl chloride	PVC	1307	pellet lenticular	4 × 4 × 2	3.17
polyvinyl chloride	PVC	1307	pellet lenticular	8 × 8 × 2	5.04
polyvinyl chloride	PVC	1307	fragment	1−2	1.26
polyethylene terephthalate	PET	1368	pellet cylindric	3 × 2.5 × 2.5	2.66
polyethylene terephthalate	PET	1368	fragment	1−2	1.26
polyethylene terephthalate	PET	1368	fiber	diameter: 1 mm, length: 10 mm	2.15
polyethylene terephthalate	PET	1368	pellet cylindric	4 × 2 × 1.5	2.29

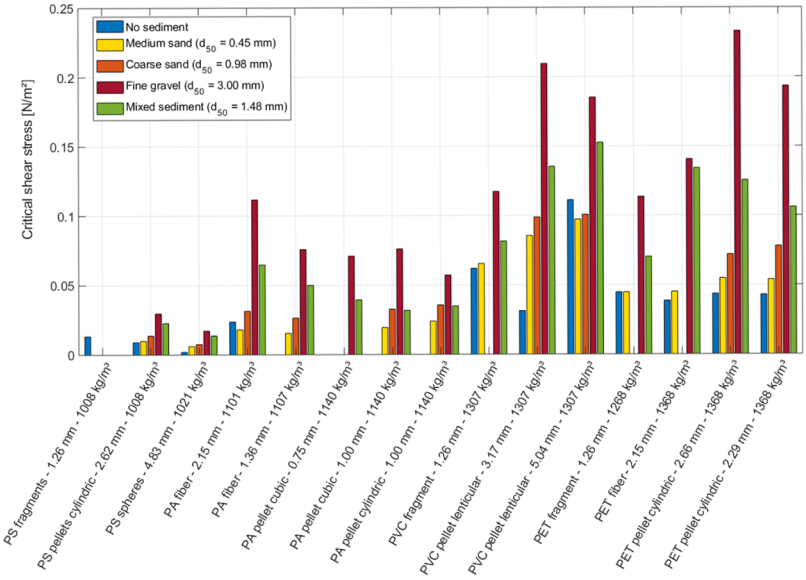

Figure 4. Graphical representation of the experimentally determined critical shear stresses, sorted by particle density and particle diameter.

because of the effects of particle shapes on erosion behavior and the chosen definition of incipient motion. Other definitions of the onset of erosion (e.g., Ballent et al. (2013):[19] the time at which 50% of the particles are in motion) depend on the observer's assessment of when 50% is reached, whereas in the definition used here, the start of the particle movement can be determined objectively. However, as the storage of the particle on the sediment bed has a strong effect on the onset of erosion, only the mean values of the 10 runs are used in the following. This should provide an adequate representation of the average onset of erosion. By analyzing the individual results, it was possible to verify that no systematical measurement deviation had occurred in the measurement methodology. One MP−sediment combination has a significantly higher standard deviation: the critical shear stress of PS spheres on the smooth bed deviates by 123%. This is probably because the average critical shear stress is very low (0.002 N/m^2) and thus the percentual deviations quickly reach large percentages.

Figure 4 shows a graphical evaluation of the mean values of all experiments carried out. Missing values for MP−sediment combinations are because the tests could not be carried out, as mentioned above.

Correlation between Critical Shear Stress and Particle as Well as Sediment Properties. In order to take a closer look at the influences of the individual parameters such as particle density, particle size, particle shape, and sediment type, linear regression analyses were carried out. To consider particle shape in these analyses, the Corey shape factor (CSF) was determined for all MP particles, which is calculated using the equation $\mathrm{CSF} = \frac{c}{\sqrt{ab}}$, where a, b, and c are the three main particle side lengths.[30] Table 3 gives an overview of the statistical relationships between MP and sediment properties and critical shear stresses.

Effects of Particle Density. It is striking that the critical shear stress increases with higher particle densities. The PET fiber with a nominal diameter of 2.15 mm and a density of 1368 kg/m^3 has a higher shear stress than the PA fiber with a nominal diameter of 2.15 mm and a density of 1101 kg/m^3. The cylindrical pellets of PS (1008 kg/m^3) and PET (1368 kg/m^3) with similar particle sizes also show this trend. This dependence could also be observed when analyzing the linear

DOI: 10.1021/acs.est.9b05394
Environ. Sci. Technol. 2019, 53, 13219−13227

Table 3. Regression Statistics for All Particles on Dependence of the Critical Shear Stress[a]

	linear regression				multivariable linear regression			
	D_i	CSF	ρ_p	D_{50}	D_i	ρ_p	CSF	D_{50}
n	51	51	51	51	51			
r^2	0.018	0.077	0.451	0.272	0.791			
p	0.175	0.027	4.147×10^{-8}	5.23×10^{-5}	0.0051	1.27×10^{-12}	0.041	8.93×10^{-11}

[a] n is the number of data points, r^2 is the adjusted coefficient of determination, and p is the p-value determined by the t-test. p-values < 0.001 indicate high statistical significance, p-values < 0.05 indicate statistical significance, and p-values > 0.5 indicate no statistical significance.[31]

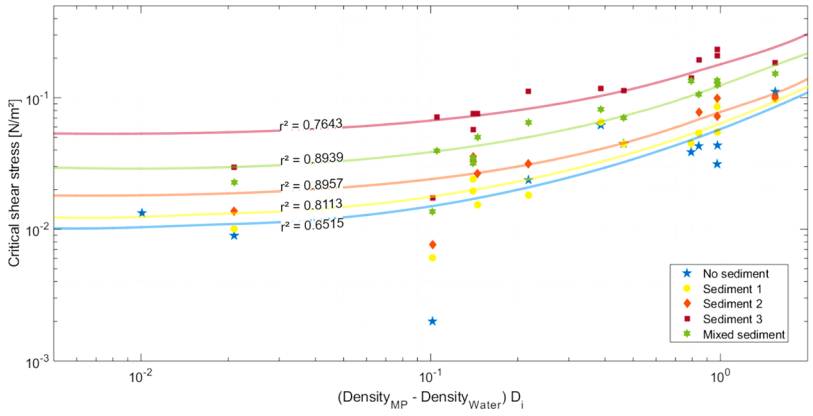

Figure 5. Critical shear stress in relation to the density difference between particle and water times particle diameter.

regression of single variables, where particle density ρ_p shows a high statistical significance ($p < 0.001$).

Effects of Particle Diameter. Particle size seems to have a lesser influence than density (p-value = 0.175 > 0.05). However, in a multivariable linear regression including D_i, ρ_p, CSF, and D_{50}, a large dependency of the critical shear stress on the considered parameters results, with an adjusted coefficient of determination r^2 of 0.791 and a high statistical significance for ρ_p and D_{50} ($p < 0.001$) and a statistical significance for D_i and CSF ($p < 0.05$). This indicates that the combination of the MP particle properties density, diameter, and shape with the sediment grain size influences the critical shear stress of MP particles severely. The lenticular PVC pellets for example have the same density but a different diameter (4 and 8 mm) and had similar critical shear stresses.

Figure 5 correlates the product of density difference between water and MP ($\Delta\rho = \rho_{MP} - \rho_w$) and diameter to the critical shear stress. In addition, the linear trend lines of the individual sediments are drawn and the coefficient of determination r^2 is given for each line. It becomes obvious that the critical shear stress τ_c is strongly dependent on $\Delta\rho x D_i$, which was expected as this relationship is also represented in the Shields diagram as the Shields parameter.

Effects of Particle Shape. In addition to the weight force, two main forces act on a particle laying on a river bed: drag and lift force. The drag force depends on the shear stress, which is a force per surface, and is thus directly dependent on the geometry of the particle. The flow-induced lift force is proportional to the particle surface exposed to the flow and thus also depends on the geometry of the particle.[21] Accordingly, the erosion behavior of the particle should be dependent on the particle shape.

However, considering the CSF in the regression analysis, a lower statistical significance of dependence of the critical shear stress on the particle shape was found (0.001 < p-value = 0.0416 < 0.05). It seems that the influences of particle density and size as well as the sediment bed cover the effects of the particle shape. To avoid this interference, PA pellets with different shapes (cylindric and cubic) but the same density and size were considered. Unfortunately, they show similar shear stresses.

However, more characteristic shapes such as spheres and fibers showed clear differences in erosion behavior. In the experiments, MP particles with a spherical shape move earliest, even before pellets with smaller diameters and lower particle densities. For example, the four points in Figure 5, which are well below the other points, belong to the PS spheres. Of all particle shapes, spheres have the smallest surface contact with the underlying ground, so there is less shear resistance and therefore less drag force is required for particle movement.[21] The spheres also roll over the sediment floor instead of saltating, which would require a stronger lift force.[21] The fibers under consideration, on the other hand, exhibit comparatively high shear stresses, which, as observed in the video recordings, was because they get caught in the sediment interspaces. According to this, the drag force seems to be more important for the erosion of round particles and the lift force more important for fibrous particles.

However, as these dependencies could not be verified with a high statistical significance in the regression analyses, further experiments with a wider range of particles should be carried out to prove the hypothesis that particle shape has a significant influence on the erosion behavior.

Effects of the Sediment Bed. When looking at Figure 4, it becomes clear that a coarser sediment leads to larger critical shear stresses for all MP particles, as fine gravel shows the highest shear stresses. In addition, it can be seen that the critical shear stress on the mixed bed (D_{50} = 1.48 mm) is between the shear stress on coarse sediment (fine gravel, D_{50} = 3 mm) and on medium sediment (coarse sand, D_{50} = 0.98 mm). In order to get a more detailed understanding of the effects of the hiding-exposure effect, further experiments with a

DOI: 10.1021/acs.est.9b05394
Environ. Sci. Technol. 2019, 53, 13219−13227

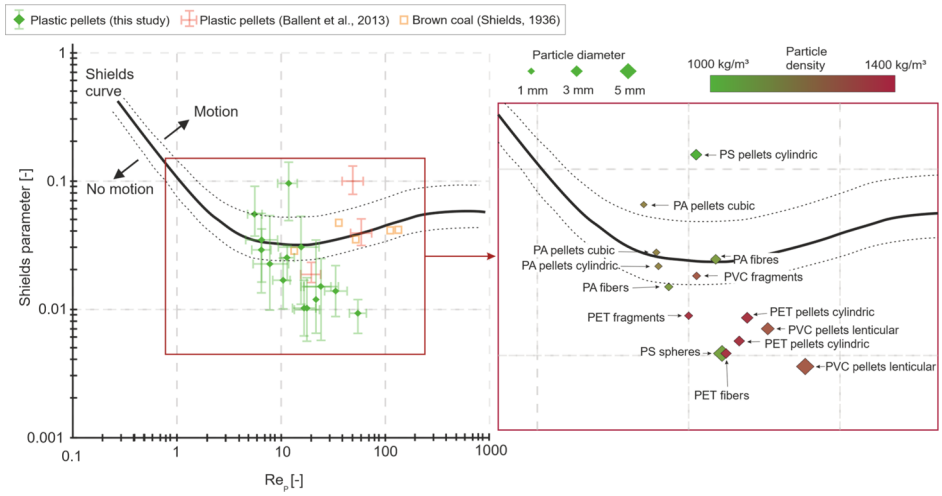

Figure 6. Left—Comparison of the test results of this study (beams show the variations between different sediment beds for each MP particle), Ballent et al. (2013)[19] and Shields (1936)[23] in a Shields diagram for uniform sediment; right—more detailed presentation of the test results of this study. Data basis in the Supporting Information, Table S4.

uniform and a mixed sediment bed with the same D_{50} would have to be carried out. Still, the size of the sediment grains D_{50} shows high statistical significances ($p < 0.001$) in the linear regression analysis, which indicated a high dependence of the critical shear stress on the underlying sediment bed.

The experiments with a smooth bottom show lower shear stresses than the experiments with sediment beds, with the exception of the PA fiber (nominal diameter: 2.15 mm) and lenticular PVC pellet (nominal diameter: 5.04 mm). On the smooth floor, the particles were more likely to slide, whereas on the sediment beds, they were more likely to move via jumping or saltating; thus, the drag force and not the lift force seems to be the driving influence there.

Comparison with Other Studies and Basics from Sediment Transport. So far, the erosion behavior of MP particles in an aquatic environment has only been investigated in one other study.[19] Ballent et al. (2013) looked at MP particles on a bed of MP, that is, a uniform composition, and determined critical shear stresses of MP pellets in saltwater. This investigation is suitable as an introductory consideration, but the significance for processes appearing in nature is low.[19] As, in contrast to this study, Ballent et al. (2013) only considered uniform MP beds, different definitions of the onset of erosion were used: while Ballent et al. (2013) chose the time at which 50% of the particles were in motion, here only one single particle was examined and therefore only its start of motion observed. Ballent et al. (2013) also calculated back from the prevailing flow velocities to the critical shear stresses, whereas in this study the critical shear stresses were determined directly. A comparison with the shear stresses of Ballent et al. (2013) can therefore be drawn (cf. Figure 6), but the different environments (marine vs fluvial), particle shapes (pellets vs various shapes), and definitions of the critical shear stress must be taken into account.

In the work of Shields (1936)[23] on sediment resuspension and transport in unidirectional water streams, particles with MP-like densities and sizes like brown coal (1.27 g/cm^3, diameter 1.77, 1.88, and 2.53 mm) were considered. It is important to note that only uniform particle compositions of brown coal were examined and not the particle−natural sediment interaction. Figure 6 compares the shear stresses of Shields (1936), Ballent et al. (2013), and the here-determined shear stresses. For the data points of this study, the minimum and maximum shear stresses on all sediment beds were plotted. More detailed classifications of the individual results can be found in Figure S1 in the Supporting Information.

Looking at the position of the MP particles and taking into account their density and shape (cf. Figure 6 on the right), it becomes clear that the heavier polymer types (PVC and PET) tend to be classified at lower Shield parameters and higher Reynolds numbers, whereas the lighter polymer types (PS and PA) have higher Shield parameters and lower Reynolds numbers. With increasing diameters, the particle Reynolds number rises as well. The particle shape seems to have little effect here.

Almost half of the MP particles are located in the lower part of the Shields diagram, which originally indicated "no motion". Especially heavier and bigger MP particles move earlier than they were expected. When separated by sediment types (see Supporting Information, Figure S1), it becomes clear that the sediment bed also has an influence on the accuracy of the Shields diagram. For almost all particles (except for the PS pellets of 2.62 mm), the results on the coarsest sediment fit best into the Shields curve. This might be due to the hiding-exposure effect, which is why this relationship is examined in more detail below.

Consideration of the "Hiding-Exposure Effect". Taking the ratio of MP particles to sediment grain size (D_i/D_{50}) into account, it can be observed that particles with particularly large ratios correspond to those that deviate strongly from the Shields curve as seen in Figure 6 (cf. Supporting Information, Table S3 and Figure S1). Ratios > 1 describe that the MP particles are larger than the sediment grains and therefore more exposed. Therefore, on the basis of the hiding-exposure effect, it can be assumed as well as seen in the experimental results that they move earlier than determined by the Shields diagram. Ratios < 1, on the other hand, indicate that the MP particles are smaller than the sediment grains and are shielded from the flow by them. Therefore, they are supposed to move later than predicted by the Shields diagram. This effect could not be clearly demonstrated in the experiments. With regard to the experimental results, it should be noted that MP−sediment combinations with a ratio close to 1, with similar particle

DOI: 10.1021/acs.est.9b05394
Environ. Sci. Technol. 2019, 53, 13219−13227

diameters of MP and sediment, are closer to the Shield curve than the others. This is not surprising as the Shields diagram was developed for uniform sediments.

For measuring the hiding-exposure effect mathematically, as mentioned above, eq 3 can be used. Therefore, the critical Shields parameter of the sediment θ_c^* must first be determined in order to calculate HE. For that, an approximation of the Shields parameter according to van Rijn (1993)[32] can be used, which is displayed in Table 4.

Without any further customization, the calculated HE values (using eq 3) for all MP−sediment combinations range between −17.18 and 5.67 and show no correlations at all. A better correlation appears when comparing the ratios of the Shields parameters of the MP and sediment ($\theta_{c,i}^*/\theta_c^*$) and the ratios of particle diameter of the MP and sediment (D_i/D_{50}). A power function fitted through all data points has a correlation coefficient r^2 of 0.7386 for all MP−sediment combinations (cf. Figure 7), which is, considering the highly variable input variables (different particle density, diameter, shape, and different sediment beds), a very suitable approximation.

Table 4. Approximation of the Critical Shields Parameter by van Rijn (1993), with $D_* = \left(\frac{\rho_s - \rho_w}{\rho_w}\left(\frac{g}{\nu^2}\right)\right)^{1/3} D_{50}$[a]

area of validity	calculation of θ_c
$1 \le D_* \le 4$	$\theta_c = 0.24 D_*^{-1}$
$4 \le D_* \le 10$	$\theta_c = 0.14 D_*^{-0.64}$
$10 \le D_* \le 20$	$\theta_c = 0.04 D_*^{-0.1}$
$20 \le D_* \le 150$	$\theta_c = 0.013 D_*^{0.29}$
$D_* \ge 150$	$\theta_c = 0.055$

[a]The Shields parameters for the used sediment beds, based on the approximations above, are displayed in Table 5.

Table 5. Calculation of Parameters for Natural Sediment Beds

	sediment 1	sediment 2	sediment 3	mixed sediment
D_{50} [m]	0.00045	0.00098	0.003	0.00148
D_* [—]	12.28	26.73	81.83	40.37
θ_c [—]	0.0311	0.0337	0.0466	0.0380
τ_c [N/m^2]	0.2267	0.5348	2.2645	0.9102
Re_p [—]	4.66	15.59	98.20	30.71

However, one MP particle (PS pellets cylindric, D_i = 2.6 mm, ρ_p = 1008 kg/m^3) showed a strong deviation from the other particles, as visualized in Figure 7 as gray data points. This deviation could be observed on all sediment beds. In the original Shields diagram, this MP particle was the only particle that was well above the Shields curve. As similar particles were examined in shape, size, and density, where no deviation was observed, the behavior of the PS pellet cannot be explained. Its data are therefore omitted from further calculation and further investigation concerning this anomaly should be conducted.

According to Figure 7, for determining the critical shear stress τ_c of different MP particles on natural sediment beds, the following equation can be used with good accuracy

$$\theta_{c,i}^* = 0.5588\theta_c^*\left[\frac{D_i}{D_{50}}\right]^{-0.503} \quad (4)$$

This equation can be used in the future to calculate the critical Shields parameter and thus the critical shear stresses of MP particles for various sediment−MP combinations without conducting experiments. The special feature is that the equation seems to be suitable for a variety of natural sediments (uniform and nonuniform) and MP particles with different shapes, densities, and sizes.

GENERAL DISCUSSION

The experiments conducted provide a first comprehensive examination of the erosion behavior of MP particles. In contrast to the previous investigation of MPs' erosion behavior,[19] the MP was eroded on natural sediment beds and different particle shapes, diameters, and densities were used, so the results are better applicable to environmental conditions.[33] Critical shear stresses for MP particles were between 0.002 N/m^2 (PS spheres on a smooth bed, D_i = 4.83 mm) and 0.233 N/m^2 (PET pellets on fine gravel, D_i = 2.7 mm), depending on particle and sediment properties. The

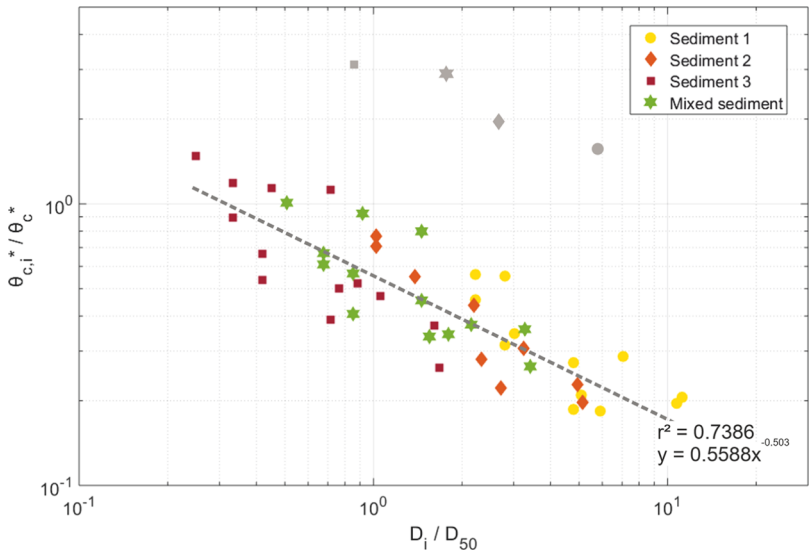

Figure 7. Ratio of Shields parameters of MP and sediment to particle diameter (trend line not including data for PS pellets cylindric, D_i = 2.6 mm (shown in gray)).

DOI: 10.1021/acs.est.9b05394
Environ. Sci. Technol. 2019, 53, 13219−13227

grain size of the sediment bed and the particle density had a particularly strong effect on the onset of erosion, as did the particle diameter and particle shape, although to a smaller extent.

A comparison with the Shields diagram has shown that half of the MP particles move earlier than expected (thus earlier than natural sediments would), and therefore a higher MP transport rate can be assumed than would be determined with the theory from sediment transport. This was explained by the impact of the hiding-exposure effect and based on the nonuniform sediment transport an adapted equation was determined, which can be used to determine the critical shear stress of MP particles on natural sediment.

What do these findings mean for further research? When considering the erosion behavior in numerical simulations, the dependence of the critical shear stress on the sediment bed has to be paid attention to and a fundamental transferability of the parameters from sediment transport to MP transport has to be rethought. This study is to be regarded as an initial examination of MP erosion in rivers, as many questions still have to be answered. Further experiments should be carried out on the effects of particle shape as well as the effects of nonuniform sediment beds on MP erosion behavior. In addition to the hiding-exposure effect mentioned above, a layer of the coarser grains forms on the surface of nonuniform sediments over time, which shields the finer sediments from the flow.[34] This armoring of the sediment bed alters the onset of erosion of the remaining particles and is therefore also of interest when investigating the erosion behavior of MP. In this context, the consequences of an infiltration of MP particles into the aquatic soil and its effects on erosion behavior should also be investigated. At last, the biological processes that might influence erosion as well, such as biofouling of the particles or biostabilization of the sediment bed, should be examined in more detail.

■ ASSOCIATED CONTENT

Supporting Information

The Supporting Information is available free of charge on the ACS Publications website at DOI: 10.1021/acs.est.9b05394.

Mean shear stress and standard deviation; standard deviation in % from mean shear stress; ratio of MP particle diameter and sediment diameter in correlation to the Shields curve; data basis, and classification of the test results in the Shields diagram with differentiations according to the sediment type and D_{50}/D_i values (PDF)

■ AUTHOR INFORMATION

Corresponding Author

*E-mail: waldschlaeger@iww.rwth-aachen.de. Phone: +49 (0) 241 80 25752. Fax: +49 (0) 241 80 25750.

ORCID

Kryss Waldschläger: 0000-0002-4120-0733

Author Contributions

The paper was written through contributions of all the authors. All the authors have given approval to the final version of the paper.

Funding

K.W. gratefully acknowledges the funding of DBU.

Notes

The authors declare no competing financial interest.

■ ABBREVIATIONS

EPS	expanded polystyrene
MP	microplastic
PA	polyamide
PE	polyethylene
PET	polyethylene terephthalate
PP	polypropylene
PP&A fibres	polyester, polyamide, and acrylic fibres
PS	polystyrene
PUR	polyurethane
PVC	polyvinyl chloride

■ REFERENCES

(1) Duis, K.; Coors, A. Microplastics in the aquatic and terrestrial environment: sources (with a specific focus on personal care products), fate and effects. *Environ. Sci. Eur.* **2016**, *28*, 2.

(2) Hurley, R. R.; Nizzetto, L. Fate and occurrence of micro(nano)-plastics in soils: Knowledge gaps and possible risks. *Curr. Opin. Environ. Sci. Health* **2018**, *1*, 6−11.

(3) Law, K. L.; Moret-Ferguson, S.; Maximenko, N. A.; Proskurowski, G.; Peacock, E. E.; Hafner, J.; Reddy, C. M. Plastic accumulation in the North Atlantic subtropical gyre. *Science* **2010**, *329*, 1185−1188.

(4) Moore, C. J.; Moore, S. L.; Leecaster, M. K.; Weisberg, S. B. A Comparison of Plastic and Plankton in the North Pacific Central Gyre. *Marine Pollut. Bull.* **2001**, *42*, 1297−1300.

(5) Baldwin, A. K.; Corsi, S. R.; Mason, S. A. Plastic Debris in 29 Great Lakes Tributaries: Relations to Watershed Attributes and Hydrology. *Environ. Sci. Technol.* **2016**, *50*, 10377−10385.

(6) Lechner, A.; Keckeis, H.; Lumesberger-Loisl, F.; Zens, B.; Krusch, R.; Tritthart, M.; Glas, M.; Schludermann, E. The Danube so colourful: a potpourri of plastic litter outnumbers fish larvae in Europe's second largest river. *Environ. Pollut.* **2014**, *188*, 177−181.

(7) Dris, R.; Gasperi, J.; Saad, M.; Mirande, C.; Tassin, B. Synthetic fibers in atmospheric fallout: A source of microplastics in the environment? *Marine Pollut. Bull.* **2016**, *104*, 290−293.

(8) Gasperi, J.; Wright, S. L.; Dris, R.; Collard, F.; Mandin, C.; Guerrouache, M.; Langlois, V.; Kelly, F. J.; Tassin, B. Microplastics in air: Are we breathing it in? *Curr. Opin. Environ. Sci. Health* **2018**, *1*, 1−5.

(9) Eerkes-Medrano, D.; Thompson, R. C.; Aldridge, D. C. Microplastics in freshwater systems: a review of the emerging threats, identification of knowledge gaps and prioritisation of research needs. *Water Res.* **2015**, *75*, 63−82.

(10) Wagner, M.; Scherer, C.; Alvarez-Muñoz, D.; Brennholt, N.; Bourrain, X.; Buchinger, S.; Fries, E.; Grosbois, C.; Klasmeier, J.; Marti, T.; et al. Microplastics in freshwater ecosystems: what we know and what we need to know. *Environ. Sci. Eur.* **2014**, *26*, 12.

(11) Khatmullina, L.; Isachenko, I. Settling velocity of microplastic particles of regular shapes. *Marine Pollut. Bull.* **2017**, *114*, 871−880.

(12) Waldschläger, K.; Schüttrumpf, H. Effects of Particle Properties on the Settling and Rise Velocities of Microplastics in Freshwater under Laboratory Conditions. *Environ. Sci. Technol.* **2019**, *53*, 1958−1966.

(13) Klein, S.; Worch, E.; Knepper, T. P. Occurrence and Spatial Distribution of Microplastics in River Shore Sediments of the Rhine-Main Area in Germany. *Environ. Sci. Technol.* **2015**, *49*, 6070−6076.

(14) Rochman, C. M. Microplastics research-from sink to source. *Science* **2018**, *360*, 28−29.

(15) Lebreton, L. C. M.; van der Zwet, J.; Damsteeg, J.-W.; Slat, B.; Andrady, A.; Reisser, J. River plastic emissions to the world's oceans. *Nat. Commun.* **2017**, *8*, 15611.

(16) Hurley, R.; Woodward, J.; Rothwell, J. J. Microplastic contamination of river beds significantly reduced by catchment-wide flooding. *Nat. Geosci.* **2018**, *11*, 251.

(17) Alimi, O. S.; Farner Budarz, J.; Hernandez, L. M.; Tufenkji, N. Microplastics and Nanoplastics in Aquatic Environments: Aggrega-

tion, Deposition, and Enhanced Contaminant Transport. *Environ. Sci. Technol.* **2018**, *52*, 1704−1724.
(18) Nizzetto, L.; Bussi, G.; Futter, M. N.; Butterfield, D.; Whitehead, P. G. A theoretical assessment of microplastic transport in river catchments and their retention by soils and river sediments. *Environ. Sci. Proc. Imp.* **2016**, *18*, 1050−1059.
(19) Ballent, A.; Pando, S.; Purser, A.; Juliano, M. F.; Thomsen, L. Modelled transport of benthic marine microplastic pollution in the Nazaré Canyon. *Biogeosciences* **2013**, *10*, 7957−7970.
(20) Besseling, E.; Quik, J. T. K.; Sun, M.; Koelmans, A. A. Fate of nano- and microplastic in freshwater systems: A modeling study. *Environ. Pollut.* **2017**, *220*, 540−548.
(21) Malcherek, A. *Sedimenttransport und Morphodynamik. Vorlesungsskript*; Universität der Bundeswehr München: München, 2009.
(22) Le Roux, J. P. Grains in motion: A review. *Sediment. Geol.* **2005**, *178*, 285−313.
(23) Shields, A. Anwendung der Ähnlichkeitsmechanik und der Turbulenzforschung auf die Geschiebebewegung. Doctoral Thesis, Technical University Berlin, Berlin, 1936.
(24) Thomsen, L.; vanWeering, T.; Gust, G. Processes in the benthic boundary layer at the Iberian continental margin and their implication for carbon mineralization. *Prog. Oceanogr.* **2002**, *52*, 315−329.
(25) Wilcock, P. R. Methods for estimating the critical shear stress of individual fractions in mixed-size sediment. *Water Resour. Res.* **1988**, *24*, 1127−1135.
(26) Zhang, H. Transport of microplastics in coastal seas. *Estuarine, Coastal Shelf Sci.* **2017**, *199*, 74−86.
(27) Kooi, M.; Besseling, E.; Kroeze, C.; van Wenzel, A. P.; Koelmans, A. A. *Modeling the Fate and Transport of Plastic Debris in Freshwaters: Review and Guidance: Freshwater Microplastics*; Wagner, M., Lambert, S., Eds.; Springer, 2018.
(28) Spork, V. Erosionsverhalten feiner Sedimente und ihre biogene Stabilisierung, 1. Aufl. *Mitteilungen/Institut für Wasserbau und Wasserwirtschaft, Rheinisch-Westfälische Technische Hochschule Aachen 114*; Academia Verl.: St. Augustin, 1997.
(29) Wadell, H. Volume, Shape, and Roundness of Rock Particles. *J. Geol.* **1932**, *40*, 443−451.
(30) Dietrich, W. E. Settling velocity of natural particles. *Water Resour. Res.* **1982**, *18*, 1615−1626.
(31) Zhu, W. p < 0.05, < 0.01, < 0.001, < 0.0001, < 0.00001, < 0.000001, or < 0.0000001 ...p. *J. Sport Health Sci.* **2016**, *5*, 77−79.
(32) van Rijn, L. C. *Principles of Sediment Transport in Rivers, Estuaries and Coastal Seas*; Aqua Publications: Amsterdam, 1993.
(33) Chubarenko, I.; Stepanova, N. Microplastics in sea coastal zone: Lessons learned from the Baltic amber. *Environ. Pollut.* **2017**, *224*, 243−254.
(34) Ferdowsi, B.; Ortiz, C. P.; Houssais, M.; Jerolmack, D. J. Riverbed armouring as a granular segregation phenomenon. *Nat. Commun.* **2017**, *8*, 1363.

DOI: 10.1021/acs.est.9b05394
Environ. Sci. Technol. 2019, 53, 13219−13227